Investigations into Dust Waste Treatment for Nuclear Fusion

Thomas Stokes*, William Grove, James Bromley, Daniella Heristchian, Stephen Reynolds

United Kingdom Atomic Energy Authority, Culham Science Centre, Abingdon, Oxon, OX14 3DB, United Kingdom

*E-mail: tom.stokes@ukaea.uk

Investigations into Dust Waste Treatment for Nuclear Fusion

The generation and accumulation of dust in future nuclear fusion reactors pose challenges related to safety, waste management and environmental impact. Dust, flakes and droplets form because of plasma-facing component erosion, with highly tritiated and activated materials accumulating in-vessel and during decommissioning activities. Estimations for dust generation in ITER predict substantial quantities of tungsten, stainless steel and boron-based particulates, raising concerns about tritium retention, dust mobilization and disposal constraints. This study details inactive trials for two treatment strategies for managing dust waste: high temperature baking and metal melting. Thermal processing was first examined through thermal treatment trials, analysing the oxidation and adhesion behaviours of ITER relevant dusts under air and inert gas conditions. Trials in the Materials Detritiation Facility (MDF) tested the viability of using dust containment baskets to facilitate high-temperature processing while minimising contamination spread. Parallel to this, metal melting via Vacuum Induction Melting (VIM) was explored as a method for consolidating fine dusts into ingots, mitigating dispersal risks. The results of this work indicate that oxidation affects dust morphology, potentially influencing both reactor maintenance and waste processing. Dust baskets in the MDF successfully contained dusts, although some loss and agglomeration occurred. VIM trials demonstrated that fine dusts could be incorporated into ingots. The use of metal containers to seed melting was promising. Tungsten powders were incorporated into melts of Stainless Steel and Inconel but presented challenges when mixed with copper. These findings contribute to the development of scalable, safe and efficient strategies for handling fusion dusts, supporting long term waste management solutions for nuclear fusion.

I. Introduction

During plasma operations in a fusion device, dusts (formed by physical and chemical sputtering from particle interactions with the plasma facing components (PFC)), flakes (broken layers of depositional films) and droplets (solidification of liquid droplets ejected by melt pools created on PFC surfaces) are formed when plasma facing components are eroded by ions and neutral particles from the plasma. This material is deposited on the plasma facing components and directly in the divertor region at the bottom of the tokamak [1][2]. The dusts generated in future fusion reactors are likely to be highly tritiated, highly activated first wall materials.

At the Joint European Torus (JET), over the lifecycle of JET approximately 400 g of dust and flake samples have been retrieved [3]. This was predominantly C based dust and flakes. It is estimated that approximately 6 kg of dust material remains in the vessel, which will be removed during decommissioning. Particle sizes for dust and flakes retrieved from JET over its lifecycle range from nm to µm scale [2] [4] [5] [6]. Tritium activities of dusts retrieved from JET are shown for various campaigns in Table 1.

Table 1. Dust and Flake activities from JET campaigns.

Campaign	**Tritium Activity**	
	Dust	Flake
Deuterium Tritium Experiment 1 (DTE-1)	560 – 1270 GBq/g[5]	1170 ± 110 GBq/g [5]
JET-C Mk-II GB	9 ± 6.75 MBq/g [4]	5.9 – 22.3 GBq/g [5]
JET-C Mk-II HD	5 – 2600 MBq/g [5]	-
ITER-Like Wall (I-LW)	6 – 750 MBq/g [5]	-

Dose rates for the dusts generated pre-I-LW (ITER-Like Wall) (1983 – 2009) range from 3 – 10 µSv/hr. Dose rates for dusts generated with the I-LW configuration from tritium operations were not available at time of writing.

In the International Thermonuclear Experimental Reactor (ITER), a full metal wall utilising

tungsten (W) and stainless steel (SS) will be used, with Boron (B) compounds also found in the vessel [7]. Experience from JET, when switching from a C first wall to the I-LW, showed a reduction in dust production by two orders of magnitude over 20 hours of plasma operation [2] [8]. Although less dust is produced in full or partly metal machines in comparison with C based fusion devices, due to the higher energy loads onto the plasma facing components and the longer pulses at ITER, the number of depositional layers, dust, and flakes generated during operations will increase significantly when compared with JET. Prior to the recent change in first wall materials (where beryllium (Be) was considered as a first wall material), it was estimated that ~ 130 kg of W and ~110kg of Be dusts would be generated during an operational DT campaign scenario in ITER [9]. Recent estimates for dust generation from ITER, post the change in first wall material, are given in Table 2.

Table 2. Predicted dust generation for ITER [7].

Phase	Process	Dust Species	Dust Weight (g)
DT-1	Boronization	B compounds	15,000
DT-1	Plasma – Wall interactions	W	21,000 (+ 27,000 for disruptions)
DT-1	Plasma – Wall interactions	SS316L	32,500

Table 2 gives values of dust generation in the vessel for “Disruption” and “No Disruption” scenarios. Disruption scenarios are events where machine components are exposed to excessive heat loads and electromagnetic forces caused by plasma disruptions, where stored thermal and magnetic energy is lost [10].

Additionally, dusts are generated during waste processing of fusion plant components during size reduction and dismantling. The amount of dust produced will vary depending on the material type and cutting technique used [11], [12] [13], as well as the amount of size reduction needed for components to be disposed of or further treated. In one study, for SS using plasma cutting, between 0.6 % to 5.7 % of the starting mass was captured in dust filters

during the cutting operation [12], with more dust not captured remaining in the cutting zone. Other cutting techniques displayed higher values still [13]. Therefore, significant volumes of activated and tritiated dusts will be generated over the lifecycle of a fusion plant. The size of these dusts is typically much larger than that of in-vessel dust, ranging from μm to mm scale, and again depends upon the cutting technique used [14].

In the ITER safety case, there are limits on the amount of mobilizable dust (1000 kg) [15] and dust deposited on hot surfaces (for W, 76 kg) [9]. This is to minimise the tritium inventory (limited to 1kg of tritium within dusts in the vessel [15]), reduce the risk of accidents (such as chemical reactions of dusts and steam from a broken cooling pipe creating hydrogen, or dust explosions [16]) and to reduce environmental release of dust [17]. There is also the concern that dust build up may impact in-vessel diagnostics [18]. Although the dust quantities are expected to remain well below the safety limits, the dust generated within the reactor needs to be managed to ensure that is the case. For the EU DEMOnstration reactor (DEMO) dust has been identified as problematic during Loss Of Coolant Accident (LOCA) due to additional mobilisation through containment levels [19].

In JET, the primary method for removing dust material is a modified vacuum cleaner, utilising the MASCOT arm operated by the Remote Applications in Challenging Environments (RACE) team. A bespoke vacuum cleaner has been fitted to the robotic arm, equipped with a cyclone filter, and specialised cyclone pots to hold the collected material [20]. At ITER, one of the primary methods for removing dust will be in-situ vacuuming whilst the divertor cassettes are being exchanged [9]. Due to the high temperatures and dose rates that will be present in the vessel, this cassette exchange and vacuuming will be undertaken by remote handling systems.

There are several factors regarding these dusts that create issues. As mentioned, the dusts

from JET are highly contaminated with tritium, and future fusion devices are expected to also have high levels of activation and absorbed tritium contamination. These high activity concentrations can be prohibitive for disposal. In addition, the small particulate size and high surface area of the dusts increases the risks of dispersal of dust into the environment via wind, leaching into water, and risk of inhalation and ingestion into humans and wildlife should primary waste containment degrade or during accident scenarios. Therefore, it is of importance that strategies are developed to also manage the volume of fines that will be generated during operation and as part of decommissioning and waste management.

At UKAEA, research has been undertaken to investigate novel methods for treating radioactive dust wastes to mitigate some of the issues previously mentioned. Research to date has primarily focused on reducing the high tritium content expected within the dust and reducing the risks associated with the particulate form through agglomeration. In this paper, inactive trials into two methods of dust treatment (high temperature baking and metal melting) are outlined and the implications of those trials discussed.

II. High temperature baking of Metal Dusts

The first set of experiments on dust focused on investigating the effects of heat treatments for detritiating dusts generated in a fusion reactor. The aim of this study was to investigate the dust behaviour at high temperatures used in thermal detritiation methods, and to see if processes such as sintering, partial melting or fusing take place. With high temperatures also exhibited in the divertor, understanding how the dusts will behave in these conditions is important, as it may also impact the ability to undertake remote maintenance and dust clean up in vessel.

The Materials Detritiation Facility (MDF) thermally treats metallic waste generated on the UKAEA site, much of which is classed as Intermediate-Level Waste (ILW) (> 12kBq/g), in

an industrial size furnace to reduce its tritium inventory below 12 kBq/g [21]. This enables processed wastes to be disposed of as Low-Level Waste (LLW), using existing disposal routes, rather than requiring long term storage and eventual disposal in a Geological Disposal Facility (GDF) as and when that becomes an option in the UK.

Sorted and segregated metallic wastes are manually loaded into the furnace and heated to temperatures of up to 1000°C under a flowing air atmosphere. The combination of heat and flowing air desorbs tritium (in the form of elemental tritium (HT) and tritiated water vapour (HTO)) from the waste material. This mixed gas stream is extracted from the furnace and passes through a catalyst to convert any HT to HTO. After passing through the catalyst, the gaseous flow enters a series of three demineralized water bubblers, where the oxidized tritium is trapped. The water bubblers capture 96 - 99% of the tritium released in the gaseous discharge [21]. The bubblers get periodically changed as the tritium inventory in the water builds up to roughly 10 GBq/litre for onward processing in a Water Detritiation System [22], where tritium is separated and recovered from the water.

The MDF has a Waste Acceptance Criteria (WAC) which prescribes what materials can be treated through the furnace. Currently, the treatment of materials is limited to only solid bulk metal or carbon-based components, and dust is listed as a prohibited material on the WAC. Having loose dust in the furnace could lead to operational issues such as dispersion and contamination of the process lines. It also leads to difficulties in clean up post operation as the dust can stick to the furnace surfaces. It is also unknown how the dust would behave at the high temperatures in the furnace. Due to the dusts large surface area and small particle size, it is unknown if interactions such as fusing, sintering and oxidation will occur which could lead to additional issues. Solutions have been proposed to alleviate this issue, such as containment or encapsulation, but to date none have been utilised.

This experiment was split into two phases. Firstly, looking at the effect of heating ITER relevant dusts at lab scale. Secondly, scaling this work up by undertaking inactive trials in the MDF furnace.

II.A. Phase 1

The aim of this experimental phase was to investigate the behaviour of relevant dusts at high temperatures, expected in vessel or in detritiation processes such as the MDF. Loose dust could lead to operational issues such as dispersion and contamination of the process lines and difficulties in clean up post operation as the dust can stick to the furnace surfaces. Therefore, the effects of high temperatures on dusts generated in a fusion reactor were investigated to see if processes such as sintering, partial melting or fusing would take place in vessel or during detritiation operations.

The dusts used in this experiment were chosen to mimic those expected to be generated during operations at ITER and were purchased from Fischer Scientific. The W powder had a particle size of 12 µm, 316L had a particle size of 44 µm and the B_2O_3 had a particle size of 400 µm. B_2O_3 is being used for B compounds in this experiment, however B metals, diborane gas or boric acid could also be present.

This work was undertaken in the UKAEA Tritium Analysis Laboratory (TAL), utilising a Raddec 6-Trio pyrolyser as the mode of heating (Figure 1). This allowed for heating up to 900°C in both air and Ar environments. Prior to the experiment taking place, the samples were photographed. The mass of the sample was also recorded. For the mixed dust experiment, the masses of each material were weighed separately prior to mixing and added together to get a total mass. The sample mass for each run was approximately 5g. The pyrolyser was heated up to 900°C and held for 2 hours utilising a flow rate of 250 mL/minute, before cooling. The experiments were repeated in air and Ar.

Figure 1. Schematic of Raddec pyrolyser.

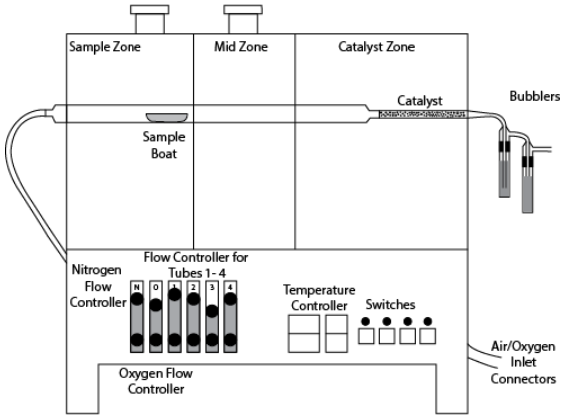

Post heating, photographs were taken of the dust samples in the pyrolyser tube and again once removed from the pyrolyser tube. The sample was also reweighed. No measurements of dust detached from the bulk/in suspension were made during this experiment. For the mixed samples, only the total mass was weighed post experiment. Following removal from the pyrolyser, the dusts were analysed by Scanning Electron Microscopy (SEM) using back-scattered electrons (BSE) to show atomic weight contrast. Energy Dispersive X-ray Spectroscopy (EDX) mapping was also used as a qualitative guide to visualise the differing relative intensities of each element within the same map. The W dusts were later analysed by Raman Spectroscopy at Imperial College London by the Materials Division of UKAEA.

The melting points of W and SS316L are 3410°C and 1375 – 1400°C respectively. These melting temperatures are higher than the maximum operational process temperature currently utilised in the MDF (1000°C) for detritiation processing and the TAL (900°C) for experimental work. Therefore, full metal melting for these materials was not expected to be observed. It is possible that in a fusion reactor divertor region, some SS dusts may melt during off-normal conditions. B_2O_3 has a melting point of 450°C and was therefore expected to fully melt when heated in the TAL. When melted, B_2O_3 forms a glassy liquid. It is therefore hypothesized that if heated with the other dusts, the B_2O_3 would encapsulate the other dust species when the liquid cools and re-forms as a solid.

It has been shown that pure W powders can enter the grain boundary diffusion process within the temperature range of 1050 – 1200°C. [25], which is outside the range of the pyrolyser used and therefore sintering of pure W is not expected in this experiment. SS sinters readily at a similar temperature range (1000 – 1100°C), with a positive correlation between heating time and density increase in a hydrogen atmosphere [23]. The large increase in density was attributed to the size of the grains used (100 nm (25%) and 4 μm (75%)). This is a scale of magnitude smaller than used in this experiment, and therefore such an increase in density is not expected here. Again, the temperatures stated cannot be reached in the pyrolyser, so sintering is not expected for the SS samples. Additionally, the dusts in the experiment were not packed into a green compact prior to heating as this step is not expected during processing. Therefore, optimal conditions to promote sintering were not employed.

Results

Pre, post and SEM images for W, SS and mixed W/SS are shown in Figure 2. The mass increase results are shown in Table 3. EDX analysis of the mixed W/SS dust post heating is shown in Figure 3. EDX analysis for W and SS is not shown as the results were inconclusive.

Mass results for heating B_2O_3 in air and Ar were unable to be recorded due to the B Oxide dust melting and forming a glass like substance that fused with the sample boats. Similarly, trials with mixed dusts and B_2O_3 were undertaken, however due to the B_2O_3 forming a glass, the mixed dust fused to the sample boat and therefore could not be weighed post operation. This also meant that SEM and EDX analysis was not possible for the mixed dusts with B_2O_3.

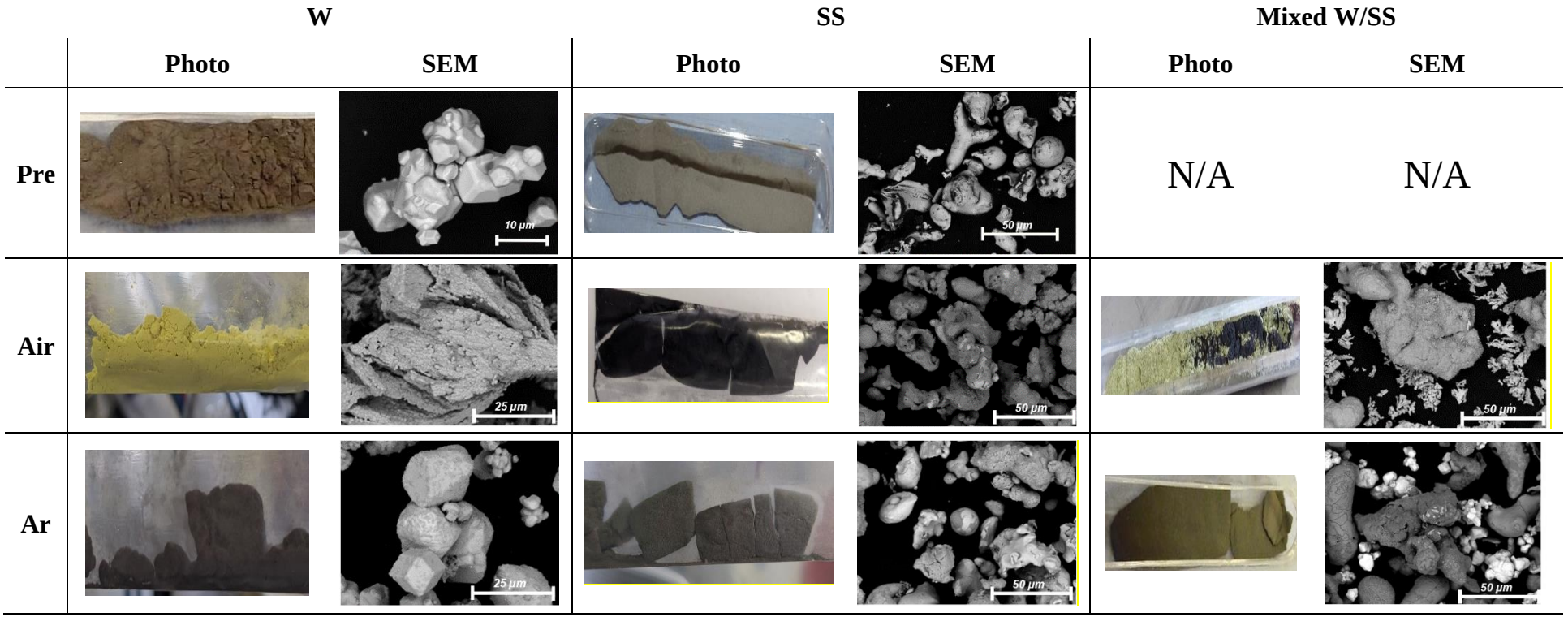

Figure 2. Photos and SEM images for the W and SS dusts pre-heating (EHT = 20kV, WD = 8.4 mm) and post heating in air and Ar (EHT = 8 – 10 kV, I Probe = 300 - 500 pA, WD = 6 – 6.5 mm) at 5.00K X Magnification.). Post-heating mixed dust BSE Images in Ar and air (EHT = 8 kV, I Probe = 500 pA, WD = 6.5 – 9.5 mm), Image width – 135 µm.

Table 3. Mass increase results for W, SS and mixed W/SS dust heating experiments.

Gas	Average Mass Increase (%)		
	W	SS	W/SS Mix
Ar	0.42	0.71	0.78
Air	24.83	3.93	25.0

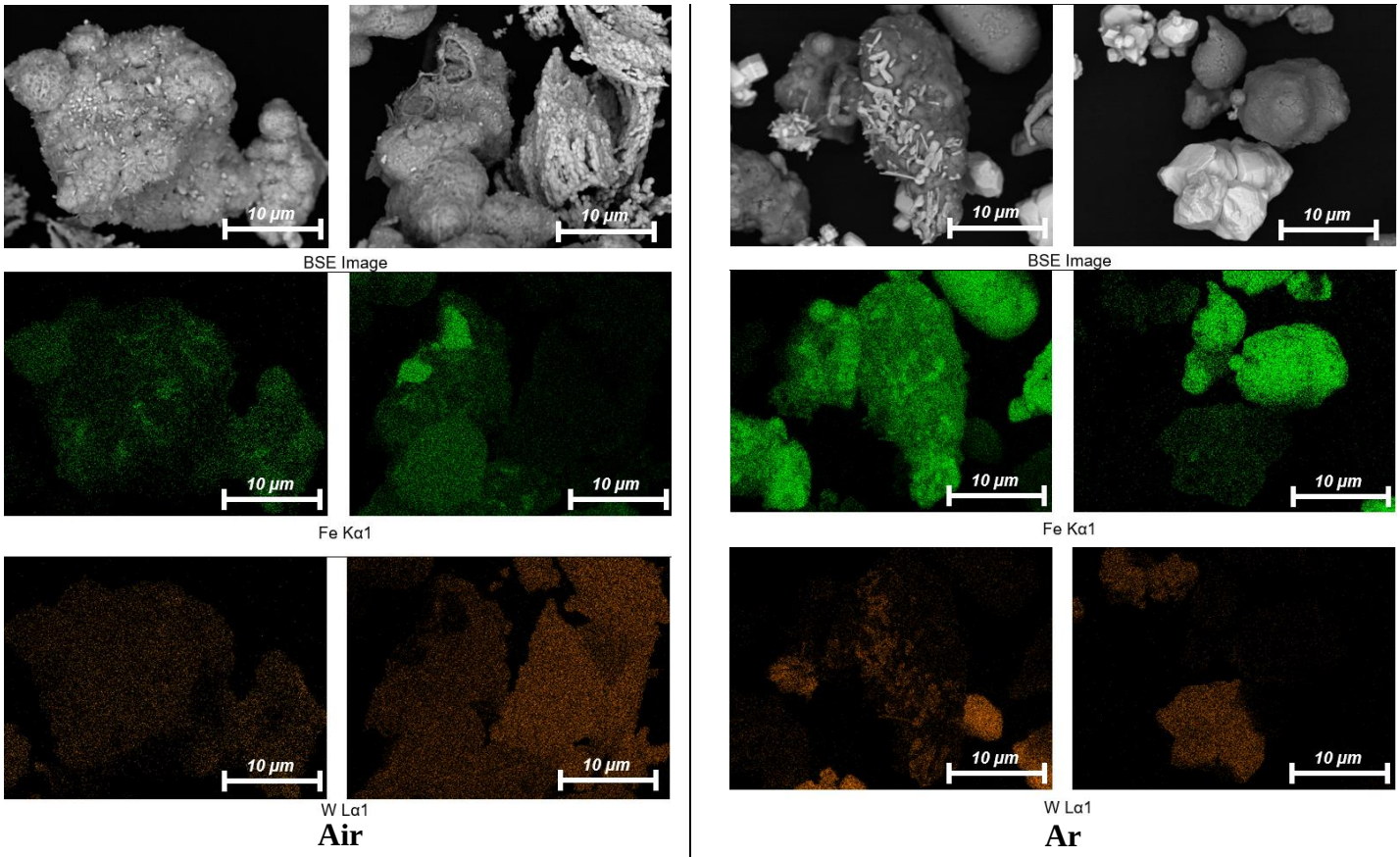

Figure 3. EDS images for dust mixture after heating in Ar. The EDS images in the left column are all from the same location shown on the left-hand BSE image. The EDS images on the right column are all from the same location shown in the right-hand BSE image. (EHT = 20kV, WD = 8.5 mm, 3 Frames).

Discussion

W showed mass increases in both air and Ar atmospheres (Table 3), relating to the formation of surface layer W oxides. In air, this oxide growth led to significant volume increases. This volume increase could lead to safety concerns when treating the dust, as any dust overflowing from the crucible or sample boat could be suspended in the interior of the oven or furnace. This would lead to an increased risk of internal deflagration, explosion and contamination of process lines. The mass increase in Ar is also from the growth of oxide layers, likely due to the presence of residual impurity levels of O in the work tube or on the surface of the dust. Oxide growth could be problematic for detritiation as oxide layers can form barriers which

can inhibit tritium release [24].

The W dust heated in air formed an oxide that caused the dust to aggregate into large agglomerations (Figure 2). Loose dust was easily eroded from these agglomerations when handled during transfer from the sample boat to a sample bag. It is possible that the oxide layer formed on individual grains grew into one another causing adhesion. Upon later inspection, these larger agglomerations of dust had broken down in the sample bag to form more, smaller, loosely joined masses and over time returned to a particulate state. The W SEM analysis demonstrates that the dust completely transforms when heated in air. The powder takes on a fibrous nature, made up on < 1 μm sized crystals. It is difficult to identify original grains due to the fibrous nature of the crystals and the large size increases caused by oxide growth. The oxides formed were confirmed via Raman Spectroscopy, which showed close peak matches regarding intensity and wavelength position for WO_3 for the W heated in air. In the event of a water based LOCA in the ITER or DEMO reactor where high temperature steam would be released into the vessel with similar oxidations reactions occurring, the complete oxidation of dust as demonstrated here would be problematic and potentially lead to blocking of secondary containment filters [19]. This needs to be considered within reactor safety cases. The EDX results for W gave no indication as to the reason for particles joining.

The W samples heated in Ar turned a dark brown colour. This was likely caused by the growth of oxides, due to residual oxygen contamination, in the form of WO_2. The WO_2 formation in Ar is expected to have occurred due to small amounts of oxygen impurity in the pyrolyser set up. Limited oxidation caused by residual oxygen impurities, which within a fusion reactor may be released during the prolonged vacuum environment the reactors are held at, does not pose an additional concern during the event of an inert gas LOCA such as

helium leak in the DEMO reactor, with the concerns remaining related to mobilisation through the containment systems.

The dusts were not packed down prior to heating, which could explain why the accumulation formed after heating in air crumbled easily when pressure was applied. Alternatively, the bonds formed between the oxide layers could have degraded once transferred, due to mechanical stress or environmental factors such as moisture weakening the bonds. The WO_3 oxide layer formed when heating in air likely inhibited the potential for sintering as the oxide layer acts as a barrier for grain diffusion. As there was significantly less oxide formed when heated in Ar, it's possible that sintering occurred between grains, causing the dust to remain agglomerated over time.

For SS, in air the dust formed a single cohesive unit which, when extracted from the sample boat for retention, remained in a single solid state. This material was very hard to the touch, although was brittle when force was applied forming straight fractures in the material (Figure 2). The colour change from a brown dust in the sample boat to a black solid mass in the sample bag is likely a patina, but this is not confirmed. In Ar, cohesion was observed between the dust particles, as evidenced by the straight cracks in the post heating photos. The SEM results show evidence for some of the larger dust particles joining together however it is inconclusive as to how they have joined. Like W, it is likely that the joining of dust particles is due to either localised, weak sintering or the interlocking of grains following grain or oxide growth.

SS showed mass increases in Ar and air respectively (Table 3), although the mass increase in air was less than seen for W, which is expected due to the oxidation resistant properties exhibited by SS. There is a clear increase in oxide formation of SS when heated in air compared with Ar. This is likely due to the increased formation of a chromium oxide passive

barrier; however, this was not proved visually or by EDS analysis. Although not detrimental when detritiating bulk pieces of metal at UKAEA, the presence of this passive chromium oxide barrier could inhibit detritiation efforts of SS dusts at high temperature due to the increase in surface area.

When heated in air, the volume of mixed dust expanded greatly so that it was overflowing the top of the sample boat. This is caused mainly by the formation of WO_3. The W and SS dusts formed a cohesive unit; however, this broke down easily when handled similarly to the pure W samples heated in air. When heated in Ar, the dust formed a solid cohesive mass in the sample boat which was solid to touch and upon moving to sample bags, this material split into segments. The SEM results in Figure 3 show evidence for the dusts binding together, with grains of W and SS joining, suggesting weak sintering, or interlocking of grains. This is particularly prevalent following the Ar heating. When heated in air, the W grains took on a more fibrous nature again when forming oxides, with small fragments of the oxidised W binding to larger SS grains. In Ar, the EDX maps clearly show W ‘spikes’ bound to larger SS grains. The EDX maps for the dust heated in air are less clear in showing the agglomeration of the two dust types but suggest a layer of W oxide coating the SS grains.

When B_2O_3 was heated in both air and Ar, the dust melted and formed a B glass which fused with the pyrolysis sample boat. This result was expected, with B_2O_3 having a melting temperature of 450°C. It is expected that H_3BO_3 would behave in a very similar way, as when heated to around 550°C it would dehydrate forming B_2O_3, which would melt as seen. For pure, amorphous B, when heated in the air to a temperature in the neighbourhood of 700°C, it inflames and burns with formation of B_2O_3 [25] and therefore is expected to behave in a similar way also. This glassy mass forming could increase the difficulty of waste management and treatment. It is expected that the ITER vessel will be baked at a few

hundred degrees as a conditioning technique routinely during operations. If the dusts are deposited at the bottom of the reactor vessel these dusts could fuse in a glassy form to the reactor vessel and require significant work to remove. Furthermore, if there is an air ingress accident scenario during operations then the same could occur. Additionally, when treating the dusts, it is likely that the separation of the B_2O_3 from the other metallic elements will be required when looking to undertake detritiation at high temperatures. The B_2O_3 could encapsulate the dust and fuse it to the detritiation vessel, again causing issues.

II.B. Phase 2

The MDF routinely only accepts bulk metallic pieces, as opposed to dust. This is because during processing, the furnace becomes a turbulent environment due to the geometry and high air flow rate. Therefore, any dust and chips loose in the furnace will be spread within the furnace, and lead to contamination spread and could lead to breakages or issues with furnace performance. Additionally, as discovered through the Phase 1 experiments, these dusts could possibly sinter and adhere to the furnace, leading to issues with clean up and long-term furnace health. Therefore, a bespoke treatment method was developed to treat the finely divided material. This involved the design and procurement of two mesh ‘Dust Baskets’, to stop the material spreading within the furnace, whilst still allowing for the air to pass over the material and promote detritiation.

The aim of this phase of experimentation was to test the effectiveness of the dust baskets in the MDF on clean dust, to determine if this methodology would be suitable for large scale dust detritiation.

The dust baskets (seen in Figure 4) are constructed from SS to ensure they do not melt at the maximum treatment temperatures within the furnace. They are identical in design, cylindrical, standing 650 mm tall with a diameter of 168 mm. The sides of the two baskets

are constructed with SS mesh of two different pore sizes, one 1µm and the other 5µm. The top and bottom of the baskets are attached via removable bolts and are also constructed with mesh to ensure air flow can occur in all directions. Prior to testing with any dust, the empty baskets were subject to a run through the MDF, to ensure they remained structurally sound. Oxide growth was seen on the mesh portion of the basket after this trial, due to the high surface area, high temperatures and oxygen rich atmosphere.

Figure 4. Images of the dust baskets used to treat the finely divided material.

For this trial, SS dust with a particle size of 44 µm was purchased from Fischer Scientific. The baskets were loaded inside an isolator, inside a fume hood, to reduce the potential spread of contamination during the loading process. For the inactive trial, both dust baskets were used. 4165.6 g were loaded into the 1 µm basket, and 4270.4 g were loaded into the 5 µm basket.

Once the material was loaded into the baskets, the baskets were loaded onto a tray and input into the furnace and treated at 1000°C with a flow rate of 350 L/min and a ramp up rate of 5°C/min. Following treatment, the baskets were removed from the furnace and the effects of the treatment process evaluated.

Results

Upon removal from the furnace, the dust baskets were weighed again. The results are shown in Table 4.

Table 4. Mass measurements for the dust baskets pre and post treatment.

Basket	Basket mass (g)	Pre-treatment dust mass (g)	Pre-treatment total mass (g)	Post treatment total mass (g)	Mass change (%)
1 µm	4165.6	997.6	5163.2	5221.6	+1.13
5 µm	4270.4	975.6	5246.0	5304.8	+1.12

Figure 5 shows some notable observations from the trial. Upon retrieval from the furnace, it was noticed that a small amount of dust had been lost during the treatment and had been deposited on the loading tray. Additionally, the dust at the bottom of the dust basket showed signs of agglomeration, like that displayed in the Phase 1 trials. A brittle, solid mass formed that had to be manually removed from the basket. It broke down into smaller clumps of dust that were also brittle. The final notable observation was the deformation of the dust baskets themselves, displayed by some of the bolt's warping following the treatment.

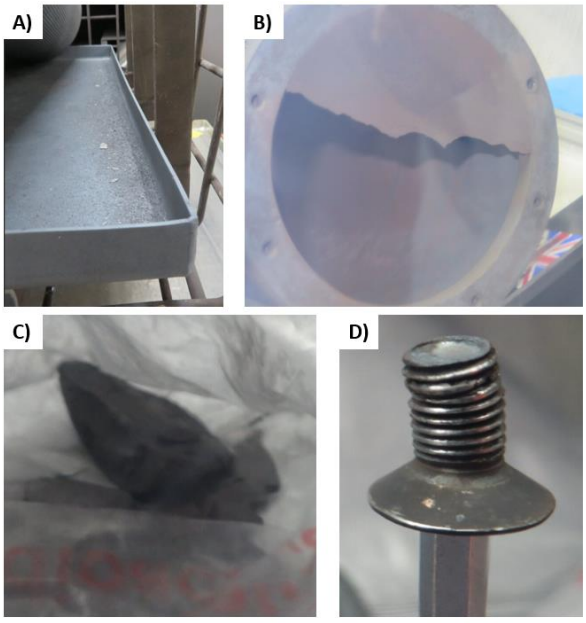

Figure 5. A) Showing loose dust in the metal tray post treatment. B) Showing the dust that had agglomerated together during treatment. C) Showing a mass of agglomerated dust post removal from the basket. D) Showing a warped bolt.

Discussion

Some dust was lost throughout the process, as shown by loose dust in the tray in Figure 5. This was not weighed following the treatment. It is hypothesized that the heat of the process caused the basket to expand, allowing for the microscale dust to escape at the seals at the top and bottom. The warping and expansion of the basket is shown by the deformation seen in the bolts used to secure the top and bottom of the mesh basket. There was also evidence of oxidation on the baskets, with a rusty red/orange colour seen on the surface. This is likely due to the mesh giving the baskets a large surface area, enhancing oxidation.

The total mass of the basket and dust increased by approximately 1% in both trials, despite dust being lost by the basket, as shown in Table 4. This is likely due to oxide growth on the dust, as indicated by the ~4% mass increase in the Phase 1 trials (Table 3). The difference between the mass gains in Phase 1 and Phase 2 could be accounted for by the mass loss through dust escaping from the dust basket. Less oxide growth is expected in the MDF treatment, as the rate of air change within the furnace is much less than in the pyrolyser, therefore the lower mass gains are not unusual. The amount of mass loss through dust escape was estimated to be < 3% based on the difference between these mass increase values.

As was seen in the Phase 1 trials, some agglomeration of the micro-scale dusts was seen, despite the dusts not being packed down into the baskets. This joining of dust particles is expected to be due to either localised, weak sintering or the interlocking of grains following grain or oxide growth, although no further analysis was undertaken. The agglomerated unit of dust was removable from the bottom of the basket, and broke into smaller masses, seen in Figure 5. This allows for the dust baskets to be re-used if deemed safe.

The agglomeration could be seen to be beneficial, as it reduces the hazardous nature of the dust being finely divided. However, only a small amount of the dust becomes fixed in the

agglomerated mass. Increasing the amount of dust agglomerated could be trialled by pressing the dusts into the baskets if this outcome was desired.

It is likely with larger dust sizes, less to no dust would escape through the expansion gaps created, and less sintering would be expected. Therefore, it is likely that this treatment method would be more suitable for treating dusts greater than micron scale.

The key aim of this trial was to test the capability of the dust baskets prior to undertaking tests with tritiated dusts, to allow for detritiation trials. The facility deemed the performance of the dust baskets to be satisfactory and tritiated dust trials will proceed utilising dusts generated by SCK-CEN during decommissioning activities [14].

III. Dust Melting

An alternative method of waste processing is metal melting. This offers the potential advantage to liberate tritium stored within the metal, whilst also reducing the volume, homogenising waste activity, and offering the ability to re-shape the waste into more packable shapes [26][27]. This is of key importance for dust, as melting fine material would provide additional benefits to detritiation in the homogenisation and consolidation of the material, thus eliminating the chance of dispersal and subsequent inhalation, ingestion, or environmental damage. The work detailed in this paper aimed to investigate the effectiveness of Vacuum Induction Melt (VIM) furnaces as a method of conglomerating dust waste from fusion, including W dusts. With a very high melting temperature (~3400°C), detritiating and consolidating W waste will be particularly challenging. Therefore, if W dust can be incorporated into melts of other materials, a combined detritiation and consolidation may mitigate some of the challenges of detritiating and safely storing this material.

VIM furnaces operate using a large induction coil supplied with alternating current (AC), that typically surrounds the workpiece held inside a refractory crucible. The AC through the coil creates an alternating magnetic field which, in turn, induces electromagnetic eddy currents in the workpiece. As the eddy currents circulate through the workpiece, they produce heat via resistive losses (Joule heating).

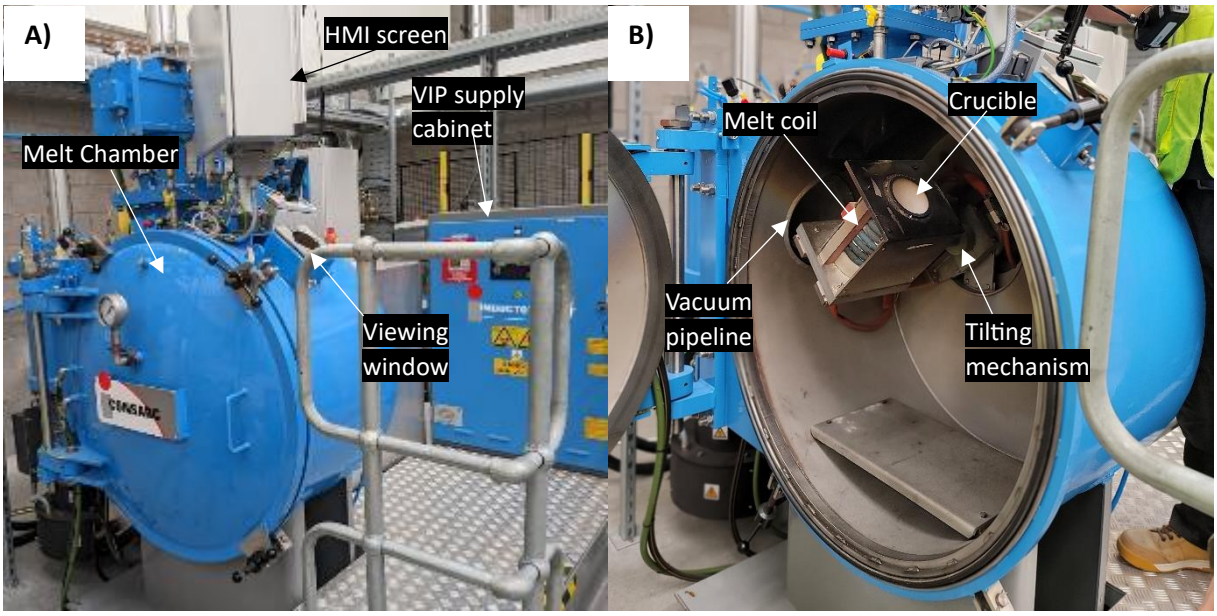

Figure 6. Front right-hand side of the rig, showing A) the melt chamber and VIP supply cabinet, and B) an inside view of the melt chamber

At UKAEA, a 4 kg capacity VIM furnace has been installed to undertake trials on bulk and particulate materials (Figure 6), supplied by Consarc Engineering Ltd. The melting coil is powered by an Inductotherm variable induction power (VIP) unit capable of supplying up to 20kW with a maximum operating frequency of 10kHz, heating to 1700 °C. The melting chamber can be evacuated to the order of 10^{-3} mbar using an Edwards NES100 rotary pump and Edwards EH500 roots blower or used in high vacuum mode with the use of an Edwards nHT10 oil diffusion pump to evacuate the chamber to the order of 10^{-5} mbar. Backfill of the chamber up to 100 mbar partial pressure is possible via cylinder gas supply. Nitrogen, argon, and 2.5% hydrogen in argon cylinders were supplied by BOC.

The benefit of VIM furnaces over other furnace designs for fusion waste management is in the control of the melt chamber atmosphere. Since heat is generated electromagnetically within the sample, the melt chamber can be evacuated or backfilled with inert gases without affecting the heating properties. This is beneficial for metallic waste detritiation to avoid the formation of oxide layers from heating metals in the presence of oxygen, which have been demonstrated to inhibit the release of tritium from the metal [24] [28]. This is particularly true for W. It also allows gas mixtures including a small quantity of hydrogen to be added to the melt chamber which may further enhance detritiation via isotopic exchange reactions.

The electromagnetic and thermodynamic properties of the metal influence the heating efficiency in several ways – due to the skin effect found in induction heating. The skin effect causes the majority (63%) of the induced current to flow between the surface of the charge piece and the skin depth (δ). The skin depth depends on the electromagnetic properties of the metal and frequency of the induced field according to equation (1), where ρ is the material resistivity, f the operating frequency, and μ the magnetic permeability of the material.

$$\delta \approx \sqrt{\frac{\rho}{\mu \pi f}} \tag{1}$$

Since induction heating is caused by resistive losses to current flow, the majority of heat is generated at the 'skin' of the conductor – thus, heating of the bulk of the metal relies on thermal conduction from the skin towards the centre. Table 5 shows the minimum skin depth for three fusion-relevant metals using an operating frequency of 10kHz.

Table 5 – Skin depth calculations for some fusion-relevant metals with a 10kHz induction coil.

Even Cu, with a high conductivity, has a minimum skin depth of > 0.5mm. This was expected to present issues when attempting to melt fine material with dimensions beneath this as the induced field will not be able to effectively couple to the fine material. It was understood that bulk material may need to be added to each crucible to induce melting.

Metal	Electrical Resistivity ρ (Ω·m)	Relative Permeability μ_r (μ/μ_0)	Magnetic Permeability μ (H/m)	Maximum Frequency f (Hz)	Min. Skin Depth (mm)
SS-304	7.20E-07	1.02	1.2818E-06 (3)	10000	4.23
Cu	1.70E-08	0.999994	1.2566E-06 (4)	10000	0.66
Inconel 600	1.03E-06	1.01	1.2692E-06 (5)	10000	5.08

Therefore, a key part of this research was to understand how much bulk material was required.

III.A. Phase 1

The first phase of work investigated melting of single material types. The first material tested in this package of work was scrap steel swarf taken from an industrial steel forging company. The swarf consisted of a mixture of low alloy steel chemistries, typically containing 3% Ni, 1.5% Cr, 0.5% Mo, and 0.35% Mn, and is a good representation of fine waste in the millimetre scale that is produced in the size reduction of metallic wastes. Secondly, Atomised SS 316 powder was procured from HD Chemicals. The particle size was <45μm, with spheroidal morphology. The composition of this powder was stated as >25% Fe, >1% Cr, 10-24.99% Ni, >1% Mo, >1% Si, 0.1-0.99% Co. Finally, Cu granules with mixed particle size 3-5mm were procured. This consisted of short strips or granules of 99.99% Cu material. These materials are shown in Figure 7.

Figure 7. Examples of the fine material used in the melt trials. A) SS swarf (< 5mm), B) SS dust (< 45 μm), C) Cu granules (3 -5mm).

A range of bulk metal scrap was used in addition to the powders listed above. SS 304 and 316 were sourced in large blocks and 2-3mm plate, all size reduced so that no dimension exceeded 4cm. Cu was sourced from ~5mm busbar cut to ~2x4cm lengths. In addition, SS canisters with removable push-fit lids were procured. These were cylindrical, with diameter 7.5cm and height 15cm.

In each trial, the crucible (either Zirconia or Alumina were used, supplied by Capital Refractories) was loaded with the material, with the quantities and loading method adjusted throughout as knowledge was gained. The crucible was loaded into the melting chamber and the chamber was evacuated of air and backfilled with Argon gas. The induction coil was then powered, and the melt proceeded. Once the melt was finished, the power was switched off and the melt allowed to cool in the chamber. The crucible and ingot were then removed and analysed to see if melting had occurred.

Results

The full results for the Phase 1 trials can be seen in Table 6. In Melt 1 and Melt 2 the crucible was loaded only with swarf. The metal showed promising heating initially, but the temperature soon plateaued, and the melts were ultimately abandoned. After cooling, the swarf was removed from the crucible. It was observed to have lightly fused together into a solid, porous structure, but had not achieved full melting. The first successful melt was Melt 3, where only ~20% of the total mass was swarf. Here, the large quantity of bulk material

heated quickly, forming a melt bath which in turn melted the swarf by thermal conduction. The resultant ingot appeared well formed and generally homogenous. In Melt 4, when attempting to reduce the ratio of bulk metal at the bottom of the crucible problems were identified whereby the swarf ‘bridged’ across the crucible walls. This left a large air gap between the melt bath beneath. As the swarf above blocked site to the optical pyrometer, the metal beneath unknowingly reached very high temperatures, causing damage to the crucible.

In Melt 5, the bulk metal was placed on top of the swarf. Here, the bulk metal heated rapidly until eventually melting down through the swarf and heating this to the melt temperature as it sank down. This loading method was employed for the remaining melts. However, attempts to further reduce the ratio of bulk metal to swarf were unsuccessful in all cases. The melts using swarf compressed into SS canisters were also unsuccessful.

Table 6. Results for particulate melting trials. N = No, P = Partial, Y = Yes.

ID		Swarf Mass (kg)	Bulk Mass (kg)	Loading Procedure	Liner	Melt Success?
SS Swarf	01	0.51	0.00	Swarf only	Alumina liner	N
	02	0.46	0.00	Swarf only	Alumina liner	N
	03	0.40	1.50	~20% swarf, bulk at base	Alumina liner	Y
	04	0.49	0.94	~33% swarf, bulk at base	Alumina liner	N
	05	0.51	1.02	~33% swarf, bulk on top	Alumina liner	Y
	06	0.58	0.58	~50% swarf, bulk on top	Alumina liner	P
	07	0.58	0.58	Re-melt of melt 06	Alumina liner	P
	08	0.43	0.85	~33% swarf. Bulk consisting of 186g tin + 662g bulk	Alumina liner	P
	09	0.43	0.86	~33% swarf. Bulk consisting of 186g tin + 678g bulk	Alumina liner	P
SS Powder	10a	1.00	0.00	Powder only	Zirconia crucible	N
	10b		0.26	Single bulk piece buried in top 1/3	Zirconia crucible	Y
	11	0.93	0.19	Loaded canister with powder	Alumina liner	Y
	12	1.66	0.19	Loaded canister with powder	Alumina liner	Y
Cu Granules	13	1	0.00	Cu pellets only	Zirconia crucible	Y

Melt 10a, with SS powder only, was unsuccessful. The next melt (10b) introduced a small piece of bulk steel weighing 250g on top of 1kg of powder. Complete melting of the entire mass was achieved after 45 minutes. Melt 11 used a SS canister, and melting was successful although there was evidence that some dust had not melted, instead consolidating within the

base of the ingot. Melt 12 incorporated more dust than Melt 11 and was successful in melting and homogenizing the dust into an ingot.

The Cu granules heated very quickly, and the finished ingot appeared well formed, with no visible impurities, and all the charge appeared to have melted.

Discussion

The furnace was found to be well-equipped to melt very fine (µm scale) powders/dusts of SS, despite the particle size being well below the minimum skin depth. This was performed by introducing a small quantity of bulk SS to the melt to couple to the induced field and seed the melting process. Once the bulk steel was heated and melting, the powder conducted the heat very effectively and melted efficiently. The proportion of bulk steel to powdered steel was reduced to 10% with no inhibitive effect on the melting efficiency.

The melting of small Cu granules was tested, though these had a larger particle size (2-5mm) which was greater than the minimum skin depth of Cu (0.6mm). As such, these melted very effectively without the addition of bulk metal. This was likely due to the small size of the material – requiring little thermal conduction from the skin to the core, whilst also maintaining a minimum size of each piece above the minimum skin depth for the metal. Additionally, the morphology of this material enabled a high packing density, ensuring good thermal conduction between each individual piece. It is hypothesized that Cu dust with particle size < 0.66 mm would require some bulk metal to seed the melting process, as was seen with SS, however this requires testing.

The furnace was less effective at melting steel with morphology between the micro and bulk scale, as was identified during initial attempts to melt steel swarf. The irregular shape of each piece significantly reduced the packing density inside the crucible, which appeared to limit the conduction between charge pieces, and the resultant porous structure of compressed swarf

may have acted like a heat sink, thus drastically inhibiting melting. Even when adding bulk SS to seed the melting, a significantly larger proportion of bulk material was required to overcome the heatsinking effect of the packed swarf. The smallest proportion of bulk metal that yielded complete melting was 66% of the total mass.

During decommissioning of fusion plants, significantly greater volumes of bulk metal will be produced than dust or swarf. If bulk metal was to be detritiated and size reduced by melting, dust and swarf could likely be used as infill material – thus melting would provide a convenient route to consolidate and detritiate this material without requiring additional processing steps. The alumina liners used throughout these experiments have an internal volume of 1200cm^3. In prior experiments with cut bulk steel sections, a maximum mass of approximately 3.4kg could be loaded – equivalent to 500cm^3. Thus, approximately 700cm^3 free space is available inside the crucible into which dust or swarf could be poured.

Another strategy proposed for handling and processing metallic dusts was to first contain them inside metal canisters, which could then be placed into a crucible and melted together. Some preliminary trials were performed here, melting SS powder loaded into SS canisters. The motivation for this work was to minimise exposure hazards of tritiated dusts. When considering the handling and processing of tritiated dusts, the transport of said material must be considered at each stage and hazards reduced where possible. If tritiated dust were to be poured into crucibles from other receptacles, there would be an increased hazard of inhalation of airborne dust or risk of contamination spread to the environment. Thus, if the dust could be stored in a meltable container at the source (i.e. cutting workshop where bulk materials are size reduced, or in-vessel vacuum cleaning device containment), this hazard is reduced, whilst also providing simple transport from the source of dust generation to the melting facility.

The work performed with the SS canisters was a promising proof of concept, with Melt 12 demonstrating the capability to melt 1.662kg of SS powder, using just the mass of the canister to seed the melting.

III.B. Phase 2

The second phase of work investigated incorporating W dusts into metal ingots, using dust or bulk of other metals. The melt process undertaken was the same as detailed in Phase 1. The dusts and fine material detailed in Phase 1 were also used in Phase 2.

In addition to the fines, SS 304 bulk pieces (cut pieces, all dimensions between 3-5cm), Inconel plate (4cm x 4cm x 2mm) and Cu (2 x 4cm and 4 x 4cm sections of busbar) were tested with the W powders to test incorporation into melts with larger charge material.

Results

The full results for Phase 2 are seen in Table *7*.

Table 7. Results for melting trials incorporating W dust. N = No, P = Partial, Y = Yes.

	ID	Dust Mass (kg)	W Dust Mass (kg)	Bulk Mass (kg)	Loading Procedure	Liner	Melt Success?
SS & W	14	0.90	0.26	0.13	Steel/W powders mixed in crucible. Bulk steel placed on top.	Alumina crucible	Y
	15	0.00	0.60	2.40	Bulk steel loaded into crucible. W powder poured into base.	Alumina liner	Y
	16	0.90	0.27	0.19	Steel/W powders mixed inside steel canister. Canister lid removed from melt and replaced with equivalent mass of bulk steel	Alumina liner	Y
Inconel & W	17	0.00	0.60	2.41	Bulk Inconel loaded into crucible. W powder poured into base.	Alumina liner	Y
Cu & W	18	0	0.3	1.2	W dust loaded in base of crucible. Bulk Cu loaded on top.	Alumina crucible	P
	19	1	0.25	0	Cu chop loaded in base of crucible. W dust poured on top.	Alumina crucible	P

Melt 14 showed promising results initially. The melt heated as was typical for the steel powder. However, the melt was suspended early after reaching 1500°C as it was apparent that the crucible had fractured. After cooling, the crucible was removed, and it was identified that a mass of the metal had leaked through the cracks into the backup crucible. The ingot had a homogenous appearance, and the W dust appeared to have consolidated within it with no evidence for loose W powder in the crucible or furnace.

Melt 16 tested SS dust inside a SS canister. The canister was loaded with SS powder and W powder to keep the same proportions as in Melt 14. The melt progressed well, and heating was stopped after the pyrometer recorded a temperature of 1616°C. After cooling, the crucible was intact, and the ingot was removed. There was almost no dust or other flaked

material inside the crucible, and the ingot appeared homogenous, although some pits in the base revealed possible concentrations of solid powder consolidated within the mass.

For Melt 15, bulk SS was combined with W powder inside a flat-based alumina liner. These dusts were not mixed prior to melting to investigate if the melting process would provide adequate mixing. During the melt, the maximum temperature read by the pyrometer was 1606°C. Towards the end of the melt, once the steel was molten, the pyrometer recorded large variations in temperature. After cooling, the ingot was removed and was found to again demonstrate good consolidation of W with SS. A small quantity of dust and flaked material was present in the bottom of the crucible.

Melt 17, testing Inconel and W, proceeded well, reaching the melting temperature of Inconel in ~45 minutes, after which the material continued to heat until a maximum temperature of 1652°C was recorded. Once the melt reached above ~1600°C, small particles were observed to be ejected from the melt and stuck to the crucible walls. After cooling, the liner was removed from the furnace and the ingot removed. All the metal was consolidated, except for the small quantity of material ejected from the melt on to the sides of the liner. The ingot appeared generally homogenous, except for the top of the ingot which appeared darker and exhibited some cracks showing possible concentrations of W.

For both Melt 18 and 19, investigating Cu and W mixing, the temperature of Cu at the top of the crucible as read by the pyrometer rose quickly, reaching the melting temperature of Cu (~1080 °C) within 20 minutes. After this, the temperature plateaued for 5-10 minutes before rising in a near-linear fashion to the target temperature of 1400 °C. After cooling, the ingots were removed from their crucibles. Whilst all the Cu was melted into one solid piece, not all of it had melted completely. Beneath the ingot, a quantity of loose W powder sat in the crucible and, after striking the ingots with a rubber mallet, additional quantities of dust fell

out from the structure. 256g of loose dust was weighed from Melt 18, and 168g of dust from Melt 19 following melting, representing 85% and 67% of the initial masses of W respectively.

Discussion

The melts using SS resulted in one consolidated ingot, indicating that all the W powder had been incorporated within the base metal. Cracks, pits, and other deformations in the ingots revealed rough structures within the ingot, likely caused by concentrations of W powder that was not melted or alloyed with the SS, but at least incorporated within the melt. These were promising results, presenting a simple technique for consolidating W powder and thus also showing the potential to detritiate this material by using the VIM furnace.

The small quantity of dust and flaked material found during Melt 15 was likely formed via degradation of the crucible, as it was similar in morphology to material generated in other trials and confirmed to be ceramic. This melt demonstrated the effect of inductive stirring to mix two separate materials and produce a single consolidated ingot containing both stainless-steel and W. This is a promising result for future trials as it indicates that mixed morphologies of metals can be combined to produce homogenous ingots.

In the Inconel trial, few small particles were observed to eject from the melt. It is assumed that these were W particles or other impurities in the metals being ejected by the stirring and heat from the melt, but no further testing was performed to confirm their composition. It is possible that with further testing using different melt conditions, the ejection of these dusts could be minimised. Despite this the resultant melt showed W dusts incorporated into the ingot.

The same results were not found with Cu. Here, the inclusion of W powder inhibited the melting of Cu, and the melts demonstrated very limited mixing and consolidation of the

powder within the molten Cu with lots of loose dust found at the end of the melting process. This is likely due to the poor miscibility of W and Cu. It is thus inferred that consolidation and detritiation of W powder is likely to be far more effective if it is consolidated using melts of materials that possess some miscibility and alloy-forming properties with W such as Inconel and SS.

IV. Conclusion

The effective management of fusion dust waste is critical for the safe operation, maintenance and decommissioning of nuclear fusion reactors. Large quantities of tritiated and activated dust will be generated from the operation and decommissioning of nuclear fusion plants, a lot of which will be metallic in nature. As demonstrated in this study, this dust poses many hazards due to its high tritium retention and activation, environmental mobility and material specific behaviour under thermal treatment. Given the large quantities of dust expected in ITER and future fusion reactors such as DEMO, the development of scalable dust treatment techniques is essential.

At UKAEA, investigations into two methods of treatment of this dust have been inactively trialled, testing the methodology of baking and consolidating the dust into ingots via metal melting. Thermal processing trials demonstrated that oxidation and sintering significantly alter dust characteristics, which could impact both in-vessel maintenance and post operational waste handling. The use of dust containment baskets in the MDF allowed controlled high-temperature processing, though some limitations such as dust escape and agglomeration, require further testing and optimisation. The results indicate that thermal processing in the MDF could be more effective for larger sized dusts, as dust escape and agglomeration would not occur. This is to be trialled in upcoming experiments looking at detritiating metallic dusts.

Metal melting via VIM successfully incorporated micron scale dusts into ingots utilising small amounts of bulk material to induce the melt, reducing their dispersibility and offering a potential detritiation method simultaneously. The use of metal canisters to contain the dust and act as the bulk material points to an effective methodology for containing, transporting and treating particulate wastes via VIM. Success was found in incorporating W dusts into the melts of SS dust and bulk and Inconel bulk material, although issues were present when mixing W dusts in Cu based melts. Although the W dusts do not melt, the incorporation into the ingot in an inert environment is a promising result in reducing the hazard of this waste.

These findings present promising avenues for fusion dust waste treatment while underscoring the need for further refinement in processing techniques. With both techniques showing high detritiation efficiencies for bulk materials, research will focus on investigating the detritiation potential for dust material using these techniques whilst optimising the methodology used. These future trials will help to develop these technologies into scalable treatment methodologies for dust wastes, ensuring the sustainability and safety of fusion energy deployment.

V. Acknowledgements

This work has been carried out in collaboration with the Tritium Analysis Laboratory (TAL) and Materials Detritiation Facility (MDF) and Fusion Technology Facility (FTF) at UKAEA, whose teams provided equipment, expertise and time for carrying out these experiments safely and reliably. Raman Spectroscopy was undertaken at Imperial College London by the Materials Division at UKAEA.

The Dust Heating phase 1 work was partly funded by and undertaken in collaboration with the ITER project. The Dust Heating phase 2 work was supported by the HORIZON EUROPE Framework Programme [Titans] funded by the European Union. Views and opinions

expressed are however those of the author(s) only and do not necessarily reflect those of the European Union. The Metal Melting work was undertaken in collaboration with Eurofusion. Many thanks for the support of these organizations.

[1] S. Ratynskaia, A. Bortolon, and S. I. Krasheninnikov, “Dust and powder in fusion plasmas: recent developments in theory, modeling, and experiments,” Dec. 01, 2022, *Springer*. doi: 10.1007/s41614-022-00081-5.

[2] X. Litaudon *et al.*, “Overview of the JET results in support to ITER,” Jun. 15, 2017, *IOP Publishing Ltd*. doi: 10.1088/1741-4326/aa5e28.

[3] J. P. Coad *et al.*, “Material migration and fuel retention studies during the JET carbon divertor campaigns,” *Fusion Engineering and Design*, vol. 138, pp. 78–108, Jan. 2019, doi: 10.1016/j.fusengdes.2018.10.002.

[4] A. T. Peacock *et al.*, “Dust and Flakes in the JET MKIIa Divertor, Analysis and Results,” *Journal of Nuclear Materials*, vol. 266–269, pp. 423–428, Mar. 1999, doi: https://doi.org/10.1016/S0022-3115(98)00670-9.

[5] N. Bekris *et al.*, “Characterisation of flakes generated in JET after DD and DT plasma operations,” *Journal of Nuclear Materials*, vol. 337–339, no. 1-3 SPEC. ISS., pp. 659–663, Mar. 2005, doi: 10.1016/J.JNUCMAT.2004.09.072.

[6] E. Fortuna-Zaleśna *et al.*, “Studies of dust from JET with the ITER-Like Wall: Composition and internal structure,” *Nuclear Materials and Energy*, vol. 12, pp. 582–587, Aug. 2017, doi: 10.1016/j.nme.2016.11.027.

[7] ITER, “Maximum fuel retention and dust production foreseen for re-baselining (8PJJF4 v1.1),” ITER. Accessed: Nov. 14, 2023. [Online]. Available: https://user.iter.org/?uid=8PJJF4&version=v1.1

[8] M. Rubel *et al.*, “Dust generation in tokamaks: Overview of beryllium and tungsten dust characterisation in JET with the ITER-like wall,” *Fusion Engineering and Design*, vol. 136, pp. 579–586, Nov. 2018, doi: 10.1016/j.fusengdes.2018.03.027.

[9] M. Shimada *et al.*, “In-vessel dust and tritium control strategy in ITER,” *Journal of Nuclear Materials*, vol. 438, pp. S996–S1000, Jul. 2013, doi: 10.1016/j.jnucmat.2013.01.217.

[10] ITER Science Division, “Plasma Disruptions,” ITER Newsline. Accessed: Oct. 04, 2023. [Online]. Available: https://www.iter.org/newsline/-/3183

[11] F. G. Cesari, M. Rogante, A. Giostri Sogin SpA, and G. Conforti, “CONTAMINATED METAL COMPONENTS IN DISMANTLING BY HOT CUTTING PROCESSES,” Florida: International Conference on Nuclear Engineering, 2006. [Online]. Available: https://proceedings.asmedigitalcollection.asme.org

[12] L. Bonavigo, M. De Salve, M. Zucchetti, and D. Annunziata, “Radioactivity release and dust production during the cutting of the primary circuit of a nuclear power plant: The case of E. Fermi NPP,” *Progress in Nuclear Energy*, vol. 52, no. 4, pp. 359–366, May 2010, doi: 10.1016/j.pnucene.2009.07.009.

[13] M. A. Ebadian, S. K. Dua, and C. H. P. H. Guha, “SIZE DISTRIBUTION AND RATE OF PRODUCTION OF AIRBORNE PARTICULATE MATTER GENERATED DURING METAL CUTTING,” 2001. [Online]. Available: http://www.hcet.fiu.edu

[14] A. Vankrunkelsven, K. Dylst, and Y. D’Joos, “Tritium Release During Different Decommissioning Techniques,” *Fusion Science and Technology*, 2024, doi: 10.1080/15361055.2024.2361198.

[15] M. Nakamura *et al.*, “Study of safety features and accident scenarios in a fusion DEMO reactor,” *Fusion Engineering and Design*, vol. 89, no. 9–10, pp. 2028–2032, 2014, doi: 10.1016/j.fusengdes.2014.04.062.

[16] M. Lukacs and L. G. Williams, “Nuclear safety issues for fusion power plants,” *Fusion Engineering and Design*, vol. 150, Jan. 2020, doi: 10.1016/j.fusengdes.2019.111377.

[17] S. J. Piet, A. Costley, G. Federici, F. Heckendorn, and R. Little, “ITER tokamak dust - limits, production, removal, surveying,” in *Proceedings - Symposium on Fusion Engineering*, IEEE, 1998, pp. 167–170. doi: 10.1109/fusion.1997.687012.

[18] A. E. Costley, T. Sugie, G. Vayakis, and C. I. Walker, “Technological challenges of ITER diagnostics,” *Fusion Engineering and Design*, vol. 74, no. 1–4, pp. 109–119, Nov. 2005, doi: 10.1016/j.fusengdes.2005.08.026.

[19] D. N. Dongiovanni, T. Pinna, and M. T. Porfiri, “DEMO Divertor preliminary safety assessment,” *Fusion Engineering and Design*, vol. 169, Aug. 2021, doi: 10.1016/j.fusengdes.2021.112475.

[20] A. T. Peacock *et al.*, “Tritium Inventory in the First Wall of JET,” *Fusion Engineering and Design*, vol. 49–50, pp. 745–752, 2000, doi: 10.1016/S0920-3796(00)00340-9.

[21] M. Kresina *et al.*, “Preparation for commissioning of materials detritiation facility at Culham Science Centre,” *Fusion Engineering and Design*, vol. 136, pp. 1391–1395, Nov. 2018, doi: 10.1016/j.fusengdes.2018.05.019.

[22] X. Lefebvre, A. Hollingsworth, A. Parracho, P. Dagliesh, B. Butler, and R. Smith, “Conceptual Design and Optimization for JET Water Detritiation System Cryodistillation Facility,” *Fusion Science and Technology*, vol. 67, no. 2, pp. 451–454, 2015.

[23] J.-P. Choi, G.-Y. Lee, J.-I. Song, W.-S. Lee, and J.-S. Lee, “Sintering behavior of 316L stainless steel micro–nanopowder compact fabricated by powder injection molding,” *Powder Technol*, vol. 279, pp. 196–202, Jul. 2015, doi: 10.1016/j.powtec.2015.04.014.

[24] T. Stokes, M. Damjanovic, J. Berriman, and S. Reynolds, “Detritiation of JET Beryllium and Tungsten,” *Fusion Science and Technology*, pp. 1–7, Jun. 2023, doi: 10.1080/15361055.2023.2219826.

[25] A. E. Tutton, “The Properties of Amorphous Boron,” *Nature*, vol. 45, no. 1170, pp. 522–523, 1892.

[26] A. N. Perevezentsev *et al.*, “EXPERIMENTAL TRIALS OF METHODS FOR METAL DETRITIATION FOR JET,” *Fusion Science and Technology*, vol. 52, pp. 94–99, 2007.

[27] Inductotherm, “What is Induction.” Accessed: Feb. 03, 2025. [Online]. Available: https://inductotherm.co.uk/what-is-induction/

[28] M. Nakayama *et al.*, “Measurement of uptake and release of tritium by tungsten,” *Fusion Science and Technology*, vol. 67, no. 3, pp. 503–506, Apr. 2015, doi: 10.13182/FST14-T65.